Int. J. Multiphase Flow, Vol. 1, pp. 585–600. Pergamon Press, 1974. Printed in Great Britain.

BURN-OUT, CIRCUMFERENTIAL FILM FLOW DISTRIBUTION AND PRESSURE DROP FOR AN ECCENTRIC ANNULUS WITH HEATED ROD

P.S. ANDERSEN, A. JENSEN, G. MANNOV and A. OLSEN

Atomic Energy Commission, Research Establishment Risø, DK-4000 Roskilde (Denmark)

(Received December 26, 1973; revised March 6, 1974)

Summary

Measurements of (1) burn-out, (2) circumferential film flow distribution, and (3) pressure drop in a 17 × 27.2 × 3500 mm concentric and eccentric annulus geometry are presented. The eccentric displacement was varied between 0 and 3 mm. The working fluid was water. Burn-out curves at 70 bar are presented for mass velocities between 500 and 1500 kg/m²s and for inlet subcoolings of 10 °C and 100 °C. The film flow measurements correspond to the steam qualities x = 19 % and 24 % for the mass velocity G = 602 kg/m²s and x = 20 % and 23 % for G = 1200 kg/m²s. The influence of the circumferential rod film flow variation on burn-out is discussed.

1. Introduction

The present investigation is a part of a joint project between AEC, Risø, AB Atomenergi, Sweden and IFA, Norway, with the goal of developing reliable prediction methods based upon subchannel analysis for diabatic two-phase flows. One objective is to perform burn-out predictions in rod clusters by means of a "film-flow model" capable of taking into account variations in mass velocities and heat fluxes along the rods and also mutual interactions between the rods and between the rods and the shroud.

The present diabatic steam—water experimental programme was primarily designed to answer some basic questions on the relationship between film flow rate and burn-out under asymmetrical conditions.

Experimental film flow measurements in eccentric annuli with air—water mixtures have been reported by Butterworth [1] and Schraub *et al.* [2]. Both experimenters found that the circumferential variation in the rod film flow rate was rather small.

2. Experimental equipment and procedure

The experiments were carried out in the 0.8 MW loop of the Laboratory of Reactor Technology at KTH in Stockholm.

The annular test section consists of a directly heated 17-mm diameter

stainless-steel rod mounted inside a 27.2 mm i.d. unheated stainless-steel tube. The heated length of the rod is 3500 mm. The rod can be mounted in positions corresponding to the eccentric displacements, E = 0, 0.75, 1.5, 2.5 and 3.0 mm. The outer tube is provided with holes for spacers, axial pressure drop distribution measurements and needle contact probes.

The rod and tube films may be sucked off through perforations beginning 10 mm above the end of the heated length and extending approximately 50 mm axially.

The rod suction holes are 1.2 mm in diameter drilled in staggered rows with a pitch of 1.5 mm. The tube suction holes have a diameter of 1.6 mm and a pitch of 1.6 mm. During experimental period No. 1 the perforations

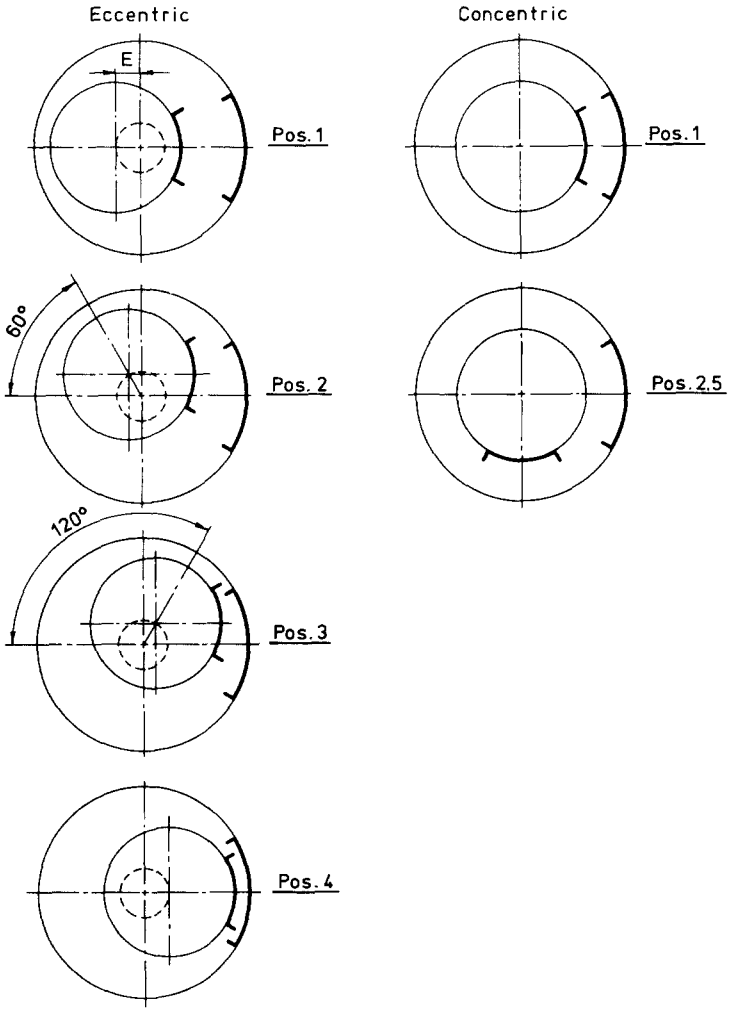

Fig. 1. Sketch of the relative positions of the rod and tube perforations. The perforated areas are indicated by the heavy line.

covered 360° of the rod and tube perimeters. During periods No. 2 and 3 the rod film perforation covered 62.3° and the tube film perforation 62.9°. The perforated areas are terminated laterally by fins extending slightly upstream and downstream of the perforations. The fin height on the tube was 1 mm. The rod fin height was 0.5 mm for experimental period No. 2 and 1 mm for period No. 3.

The steam—water mixtures extracted through rod and tube perforations were condensed in separate heat exchangers and metered by venturis or orifices. The relative amounts of steam and water were determined by heat balances, once steady state conditions had been reached in the extraction system.

The extracted fluid was returned to the suction side of the main circulator so that stable temperature and flow conditions were maintained in the test section also during the film extraction process. Under these stable conditions quality was determined at the end of the heated length by a heat balance on the test section. Rod and tube suctions were not performed simultaneously.

The relative positions of the rod and tube perforations which were realized experimentally are summarized in Fig. 1.

The spacers were 2 mm diam. pins with semispherical tips mounted radially on the tube with a distance of 500 mm between spacer levels.

There were 3 spacers per level during experimental periods No. 1 and No. 2. Because some difficulties were encountered in positioning the rod at the most eccentric positions, the design was altered to incorporate four spacers per level during experimental period No. 3.

Burn-out was determined by a bridge type detector, connected to the rod at the three upper spacer levels.

3. Results

3.1. Burn-out

Figure 2 summarizes all the burn-out measurements on concentric and eccentric annuli. The graph gives the burn-out power Q as a function of the mass flux, G, for the subcoolings $\Delta t_{sub} = 10\ ^{\circ}C$ and $\Delta t_{sub} = 100\ ^{\circ}C$. For each subcooling the eccentric displacement, E, is a parameter. It is clear that burn-out is adversely affected by eccentricity for $G > 500\ kg/m^2s$.

3.2. Film flow

In general, a two-phase mixture is being sucked out through the perforations in tube and rod. Plotting the sucked out water flow rate, m_w, versus the steam flow rate, m_s, one obtains a "suction curve" (see Fig. 3 for an example). The shape of the suction curves reflects the steam content in the film, the waviness of the film surfaces and the water content in the core. For the present purpose the "film flow rate", m_f, is defined by a straight line extrapolation of the suction curves to $m_s = 0$ (broken lines in Fig. 3).

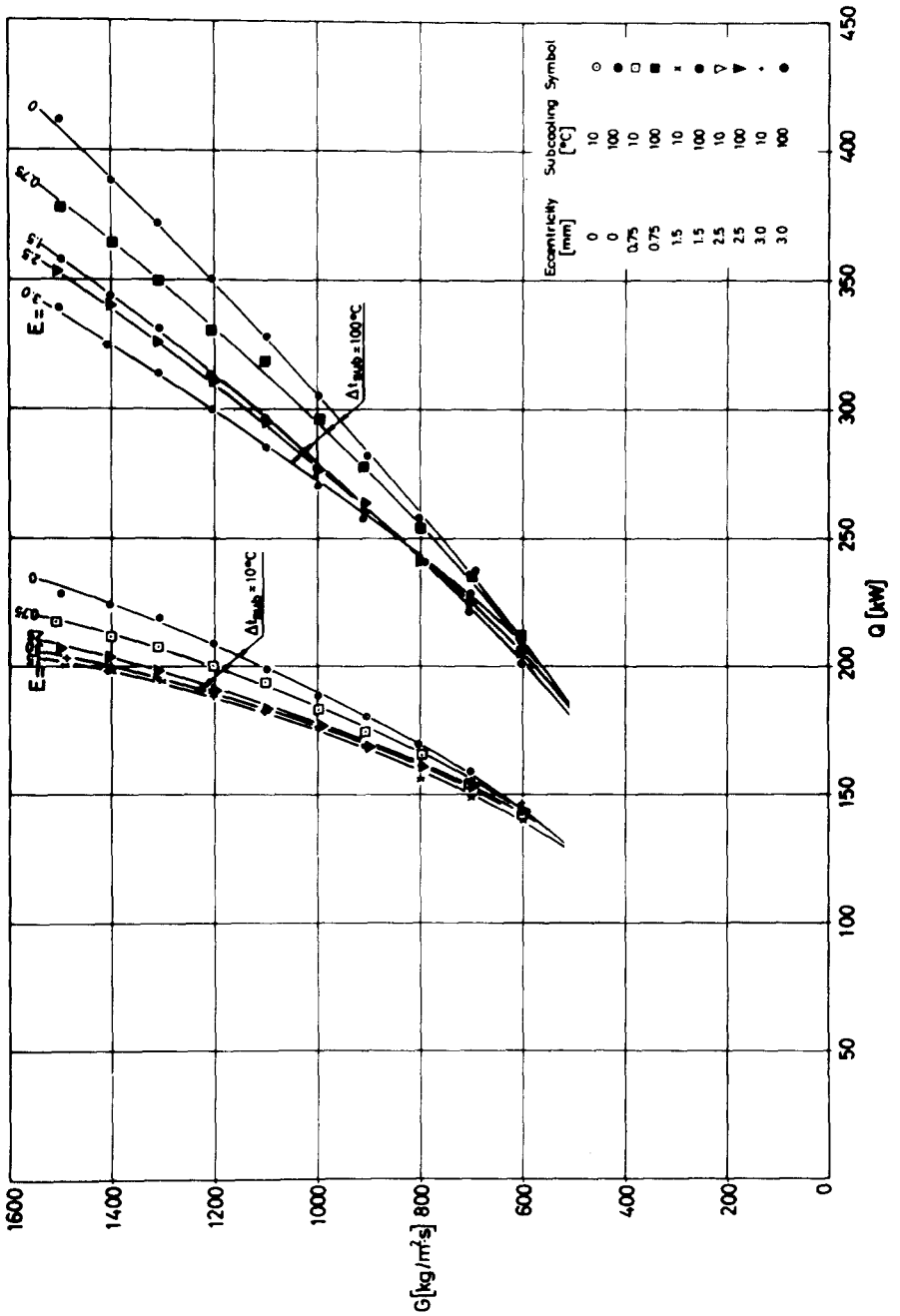

Fig. 2. Burn-out in (17 × 27.2 × 3500 mm) annulus geometry with heated rod. Burn-out power, Q, *versus* mass flux, G, for two subcoolings, Δt_{sub}, and various eccentric displacements, E.

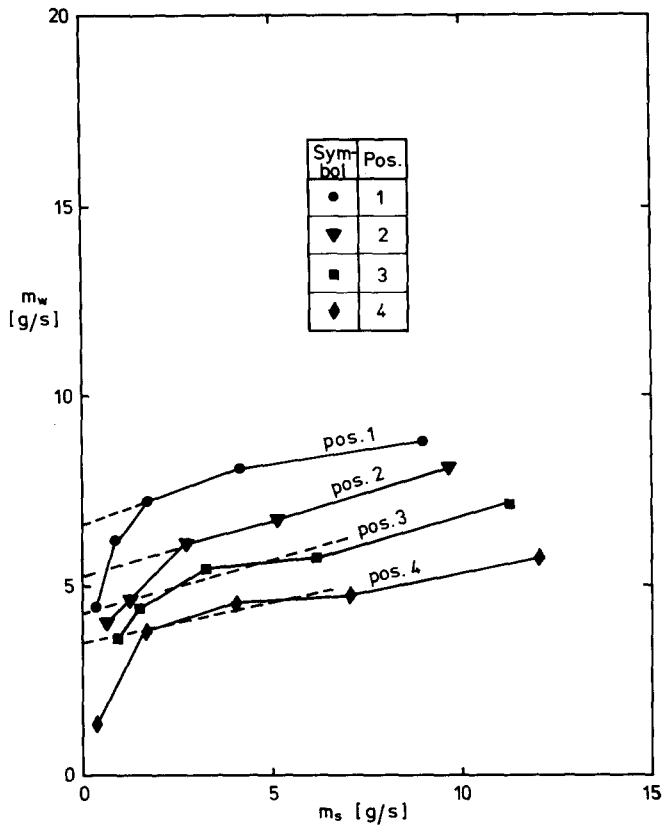

Fig. 3. Examples of "suction curves", *i.e.* sucked-off water *versus* sucked-off steam. Broken lines are straight line extrapolations to zero steam flow rate for the purpose of defining film flow. G = 1200 kg/m²s, q''_{rod} = 101 W/cm², x_0 = 22.9 % and E = 1.5 mm. Experimental period No. 3.

The experimental data for rod and tube film flow are summarized in Tables 1 and 2, respectively. The total film flow rates indicated by "Σm_f" have been computed by assuming film flow symmetry around the geometrical line of symmetry.

For a concentric configuration it was found that turning the perforation by 90° (*i.e.* from position 1 to position 2.5) does not alter the measured film flow rate. This is taken to indicate that the film is evenly distributed around the rod for concentric conditions.

However, comparing concentric suction results from a fraction of the perimeter of the rod (*i.e.* 62.3°) with results for suction from the total perimeter a difference was noted. The rod film flow rate deduced from "total suction" is inexplicably lower (by up to 30 %) than that from "partial suction" (see Table 1). It might be assumed that water deposited on the fins

TABLE 1

Rod film flow rates, p = 70 bar, q''_{rod} = 101 W/cm²

G (kg/m²s)	x_0 (%)	E (mm)	m_f (g/s) (Suction from 62.3°)					M_f (g/s)	
			Position 1	Position 2	Position 3	Position 4	Position 2.5	Σm_f	Suction from 360°
602	23.9	0	(3.6) 3.6				3.6	20.8	[16.8]
		1.5	(5.6) 5.7	(3.7) 4.8	(2.6) 3.7	(2.1) 3.0		22.2	
		2.5	6.3	4.5	2.5	1.8		21.3	
		3.0	(6.5)	(5.0)	(1.5)	(0.4)		19.2	
	19.0	0	(5.2)					30.0	[20.8]
		1.5	(7.7)	(4.7)	(2.0)	(2.0)		22.2	
		3.0	(9.2)	(5.3)	(1.0)	(1.0)		22.0	
1200	23.2	0	(5.6) 5.8				5.0	33.5	
		1.5	6.6	5.2	4.3	3.5		28.0	
		2.5	4.5	3.8	3.2	2.5		20.2	
		3.0			(3.0)				
	20.2	0	(7.4)					42.8	[30.0]
		1.5	(5.8)	(6.5)	(4.3)	(3.6)		29.9	
		3.0	(9.2)	(7.9)	(2.4)			≈28.7	

Numbers in square brackets: Exptl. period No. 1 (suction from 360°).
Numbers in parentheses: Exptl. period No. 2 (rod fin height 0.5 mm).
Other numbers: Exptl. period No. 3 (rod fin height 1 mm).

TABLE 2

Tube film flow rates, p = 70 bar, q''_{rod} = 101 W/cm²

G (kg/m²s)	x_0 (%)	E (mm)	m_f (g/s) (Suction from 62.9°)								M_f (g/s)		
			Position 1		Position 2		Position 3		Position 4		Position 2.5	Σm_f	Suction from 360°
602	23.7	0	(20.5)	21.4							19.0	120	[115]
		1.5	(24.0)	33.0	(24.0)	24.3	(16.4)	21.5	(13.5)	18.3		125	
		2.5		31.2		26.0		16.1		9.6		119	
		3.0	(29.0)		(26.4)		(15.5)		(9.0)			116	
	18.9	0	(20.6)									113	[118]
		1.5	(23.5)		(22.1)		(16.1)		(13.0)			108	
		3.0	(31.0)		(25.0)		(16.5)		(7.0)			115	
1201	23.1	0		31.0							31.0	117	
		1.5		35.0		36.5		33.0		27.0		192	
		2.5		35.4		36.4		24.8		17.3		167	
		3.0					(25.2)					—	
	20.1	0	(27.8)									159	[163]
		1.5	(39.4)		(35.0)		(29.0)		(24.3)			183	
		3.0	(35.5)		(35.5)		(23.5)		(8.0)			155	

Numbers in square brackets: Exptl. period No. 1 (suction from 360°).
Numbers in parentheses: Exptl. period No. 2 (tube fin height 1 mm).
Other numbers: Exptl. period No. 3 (tube fin height 1 mm).

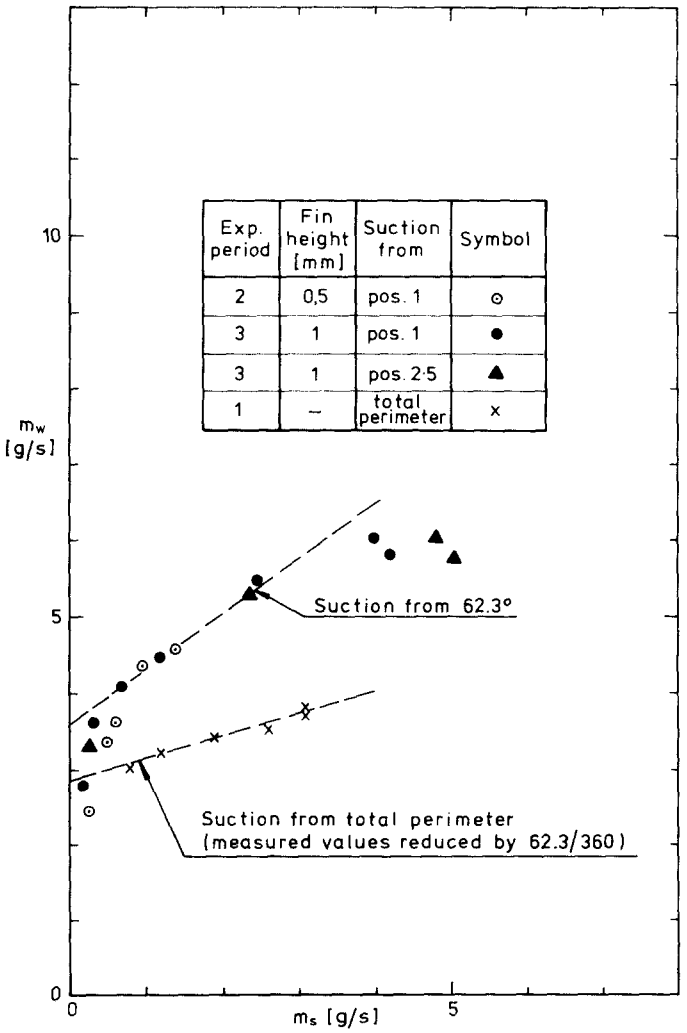

Fig. 4. Rod suction curves for concentric conditions. Comparison between suction from 62.3° with two different fin heights and suction from the total perimeter. p = 70 bar, G = 602 kg/m²s, q'' = 101 W/cm² and x_0 = 23.9 %.

accounts for the difference. However, as may be seen from Fig. 4, the two sets of fins (one 0.5 mm in height, the other 1.0 mm) gave almost identical results. Figure 5 displays the corresponding suction curves for the tube film. It may be observed that the tube suction curves for a concentric annulus from the two experimental periods are in good agreement. The measured tube film flows for the concentric condition therefore show good agreement between results obtained by "fractional suction" and suction from the total perimeter. Additional examples of the reproducibility of the suction curves

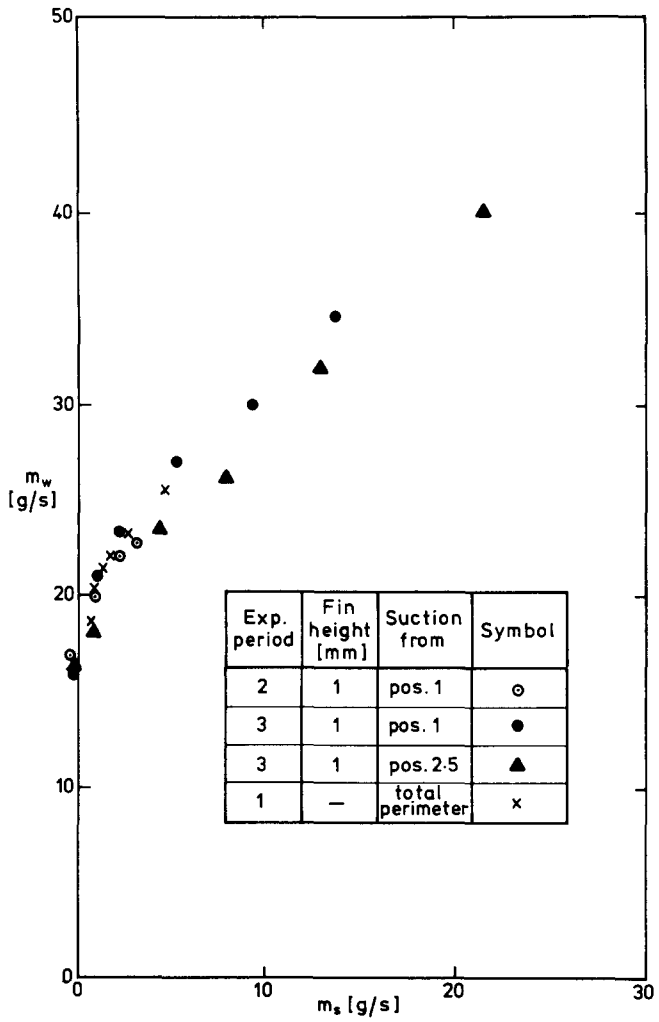

Fig. 5. Tube suction curves for concentric conditions. Comparison between suction from 62.9° and suction from the total perimeter. p = 70 bar, G = 602 kg/m²s, q'' = 101 W/cm² and x_0 = 23.9 %.

are shown in Figs. 6 and 7 for the rod and the tube, respectively. The two suction curves in the figures are from experimental periods No. 2 and 3, but correspond to the same main system parameters, namely G = 602 kg/m²s, q'' = 101 W/cm², x_0 = 24 % and E = 1.5 mm. The hatched area between the curves gives an indication of the occasionally poor reproducibility of the suction curves. Since the scatter on the measurements of m_s and m_w is only about 5 % of ($m_s + m_w$) we feel that this occasional lack of reproducibility is due to an instability in the film flow distribution itself.

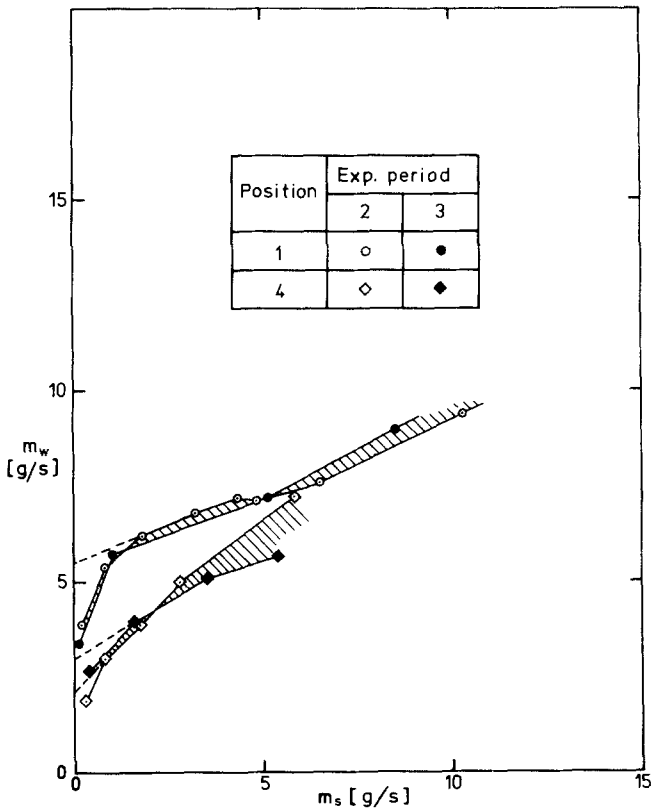

Fig. 6. Examples of the reproducibility of the rod suction curves. p = 70 bar, G = 602 kg/m²s, q'' = 101 W/cm², x_0 = 23.9 % and E = 1.5 mm.

Figure 8 presents an example of the angular variation of the rod film flow for various eccentric displacements. The film flows corresponding to suction from approximately 1/6 of the perimeter are plotted *versus* the angular position of the rod.

It is obvious that eccentricity has a very pronounced effect on the circumferential distribution of the rod film flow: the greater the eccentricity, the more uneven the film flow rate. The maximum film flow rate occurs at the maximum gap width (position 1). For the highest eccentric displacement (E = 3 mm) the minimum film flow rate occurring at the minimum gap (position 4) is relatively close to zero.

Figure 9 shows one example of the angular distribution of tube film flow for various eccentric displacements. The effect of eccentricity is almost as pronounced as for the rod film and the lowest film flow rate is also here found in the narrow gap (position 4). The total tube film flow rate is not very dependent upon eccentricity.

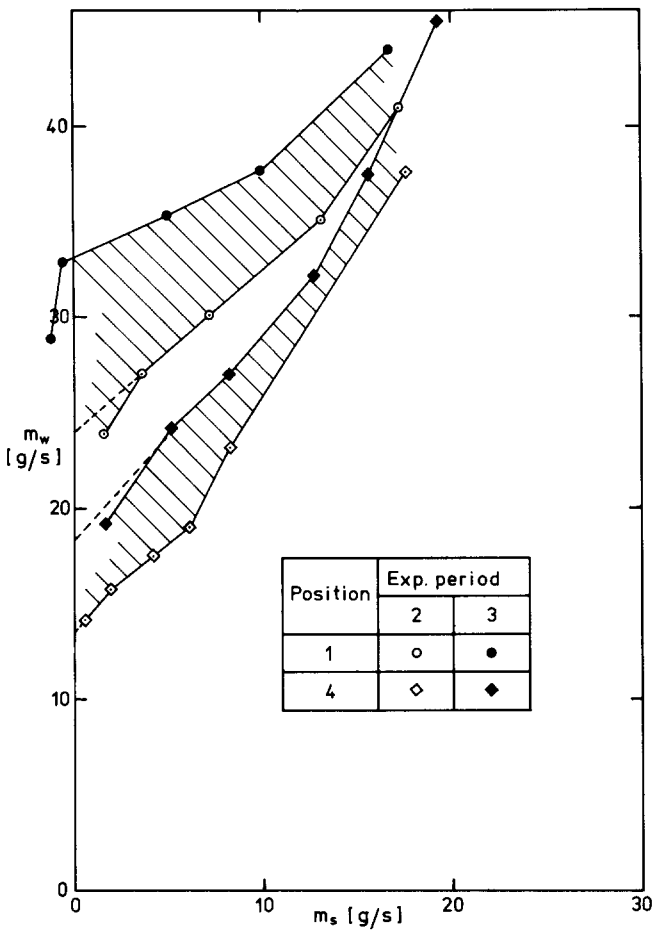

Fig. 7. Examples of the reproducibility of the tube suction curves. p = 70 bar, G = 602 kg/m²s, q'' = 101 W/cm², x_0 = 23.7 % and E = 1.5 mm.

In Figs. 10 and 11 the total rod film flow rates are displayed as a function of the steam quality, x_0, for G = 602 and 1200 kg/m²s, respectively. Also shown in these graphs are the burn-out qualities for q'' = 101 W/cm² obtained by linear interpolation in plots of measured values of x_{BO} versus q''_{BO}.

3.3. Frictional pressure drop

The two-phase frictional pressure drop was determined from the measured total pressure drop corrected for the influence of the hydrostatic head and the acceleration pressure drop by means of the Bankoff—Jones void formula,

$$S = \frac{1-\alpha}{k_s - \alpha + (1-k_s)\,\alpha^R}$$

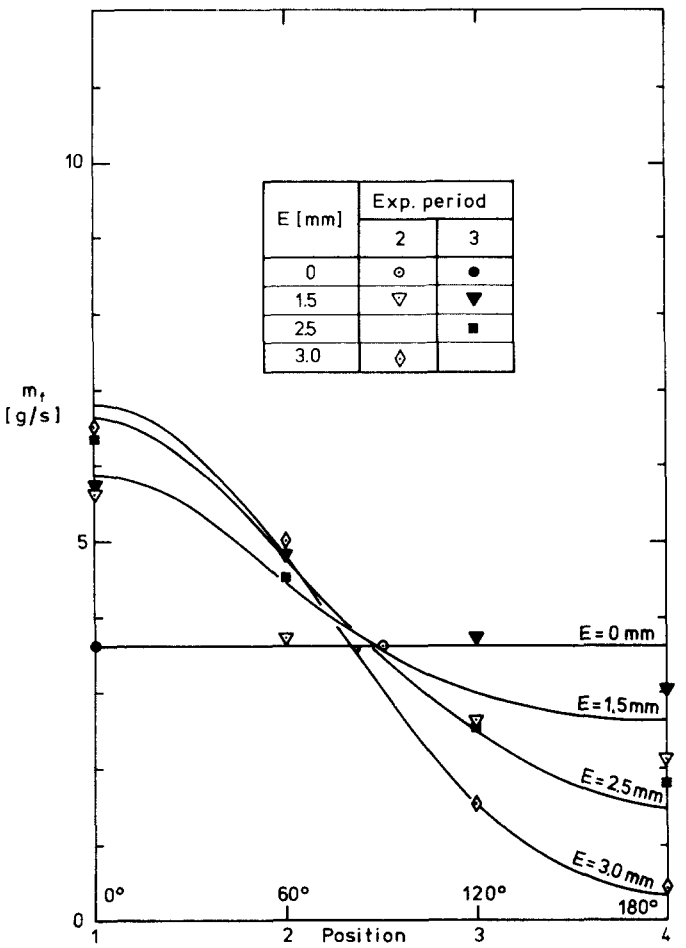

Fig. 8. Angular distribution of rod film flow rate on 62.3°. (Refer to Fig. 1 for meaning of "Position".) p = 70 bar, G = 602 kg/m²s, q'' = 101 W/m² and x_0 = 23.9 %.

with the following constants:

$$k_S = k_{BJ} + (1 - k_{BJ})p/p_{cr}$$
$$R = 3.33 + 0.0026p + 0.000097\,p^2$$
$$k_{BJ} = 0.9086\,G/(G + 123).$$

The liquid phase pressure drop as determined from measurements has been fitted by the formula

$$\left(\frac{dp}{dz}\right)_{\text{friction}} = 0.40\,\mathrm{Re}^{-0.25}\,\frac{1}{D_H}\,\frac{G^2}{2\rho_l}\,.$$

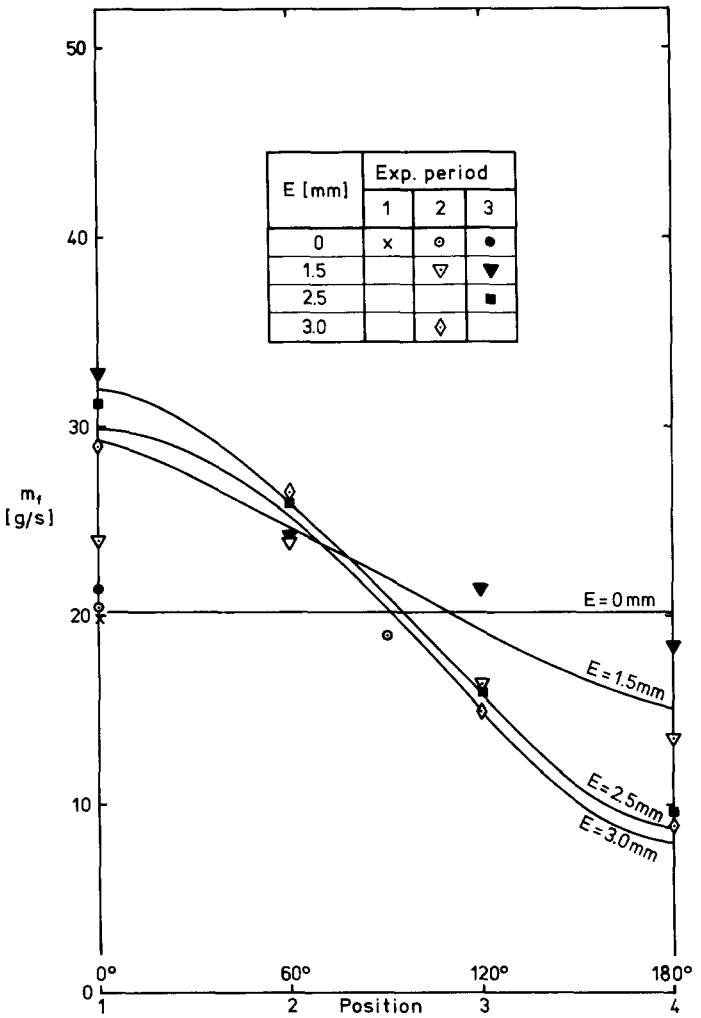

Fig. 9. Angular distribution of tube film flow rate on 62.9°. (Refer to Fig. 1 for the meaning of "Position".) p = 70 bar, G = 602 kg/m²s, q'' = 101 W/cm² and x_0 = 23.7%.

The two-phase friction multiplier, Φ^2, was defined as the ratio between the two-phase frictional pressure drop and the above fit of the corresponding liquid phase pressure drop.

The pressure drop due to the spacers was determined experimentally to be negligible both for single and for two-phase conditions.

Figure 12 gives the result of the diabatic pressure drop measurements at 70 bar for a constant heat flux of q'' = 101 W/cm² and two values of the

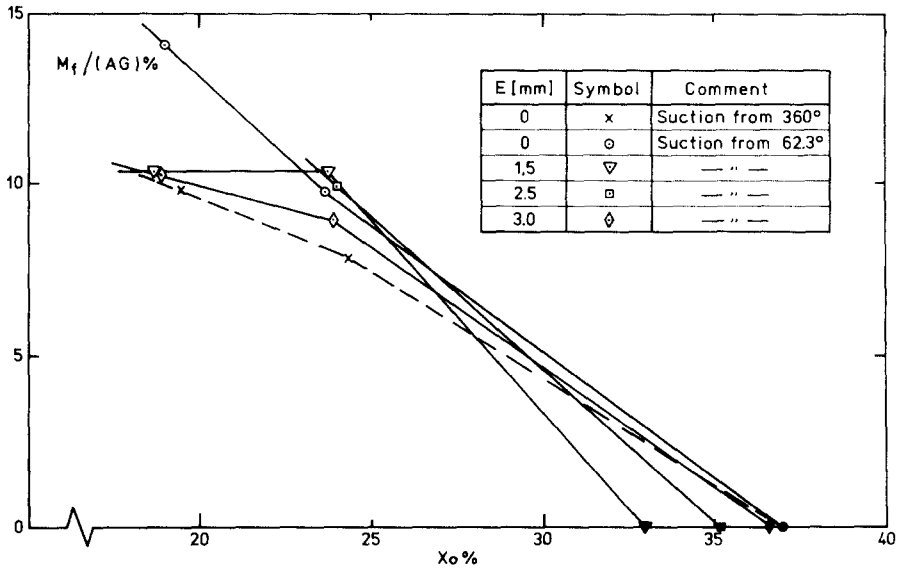

Fig. 10. Total relative rod film flow rate *versus* steam quality for various eccentric displacements. Filled symbols are interpolated burn-out results. p = 70 bar, G = 602 kg/m²s and q'' = 101 W/cm².

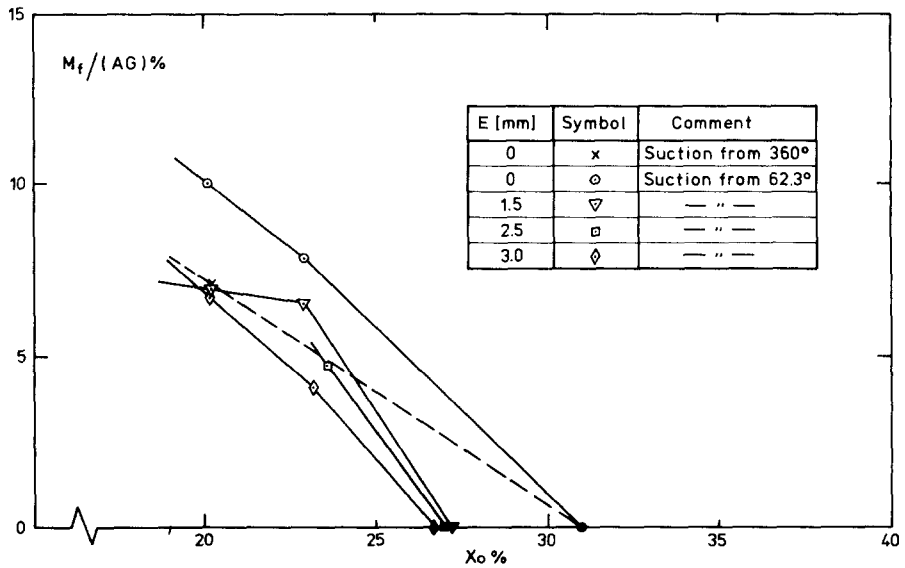

Fig. 11. Total relative rod film flow rate *versus* steam quality for various eccentric displacements. Filled symbols are interpolated burn-out results. p = 70 bar, G = 1200 kg/m²s and q'' = 101 W/cm².

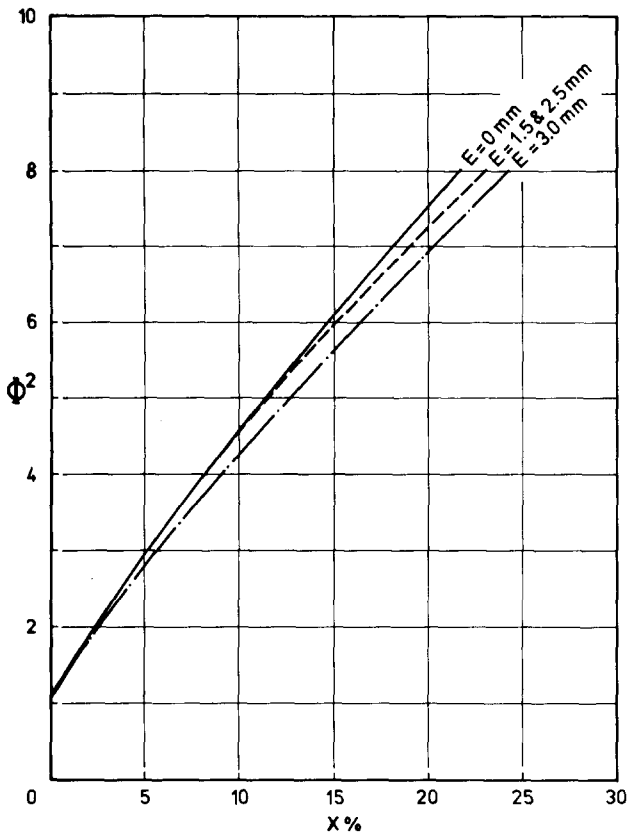

Fig. 12. Two-phase friction multiplier *versus* steam quality for various eccentric displacements. p = 70 bar, G = 600 and 1200 kg/m^{2}s, q'' = 101 W/cm^2.

mass flux, G = 600 kg/m^{2}s and 1200 kg/m^{2}s. The figures are given with the eccentric displacement, E, as a parameter. The experimental points have been omitted for clarity. The scatter of the experimental points is less than 5 % except at the low qualities.

It can be seen from the figure that the influence of eccentricity is small. However, a slight decrease in the frictional pressure drop may possibly be observed for increasing eccentricity.

4. Conclusions

Experiments with water in a 17 × 27.2 × 3500 mm concentric and eccentric annulus geometry with heated rod have led to the following conclusions:

(1) Rod eccentricity has an adverse effect on burn-out at mass fluxes greater than 500 kg/m^{2}s.

(2) The circumferential variation of the rod and tube film flow rate

becomes increasingly pronounced for increasing eccentricity. The film flow rate is smallest in the narrow gap. The rod film flow becomes close to zero at the highest eccentricity (3 mm) even at steam qualities rather far removed from the burn-out quality.

(3) The total rod film flow rate decreases with increasing eccentricity for $G = 1200$ kg/m^{2}s, but remains relatively unaffected at $G = 600$ kg/m^{2}s.

(4) Eccentricity has possibly a small (beneficial) effect on the pressure drop.

Nomenclature

A	cross-sectional area of annular test section, m^2
D_H	hydraulic diameter, m
E	eccentric displacement, mm
G	mass flux, kg/m^{2}s
M_f	total film flow rate, g/s
m_f	film flow rate ("partial suction"), g/s
m_s	steam flow rate ("partial suction"), g/s
m_w	water flow rate ("partial suction"), g/s
p	pressure, bar
p_{cr}	critical pressure, bar
Q	total rod power, kW
q''	rod heat flux, W/cm^2
$Re=GD_H/\mu$	Reynolds number
S	slip ratio
x	steam quality
x_0	steam quality at outlet
z	axial coordinate, m
Δt_{sub}	inlet subcooling, °C
α	void
ρ_l	density of liquid, kg/m^3
Φ^2	two-phase friction multiplier (ratio between frictional pressure drops of two-phase mixture and saturated water at same G)
μ	dynamic viscosity, kg/ms

References

1 D. Butterworth, Air—water climbing film flow in an eccentric annulus, U.K.A.E.A., Report No. AERE-R5787 (May 1968).

2 F.A. Schraub, R.L. Simpson and E. Janssen. Two-phase flow and heat transfer in multirod geometries. Air—water flow structure data for a round tube, concentric and eccentric annulus and nine rod bundle, GEAP-5739 (1969).